

www.acsami.org Research Article

Significantly Enhanced Thermal Conductivity of hBN/PTFE Composites: A Comprehensive Study of Filler Size and Dispersion

Liam Alexis, Jaejun Lee, Gustavo A. Alvarez, Samer Awale, Diana Santiago-de Jesus, Maricela Lizcano, and Zhiting Tian*

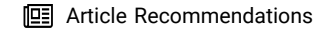


Cite This: https://doi.org/10.1021/acsami.4c03818



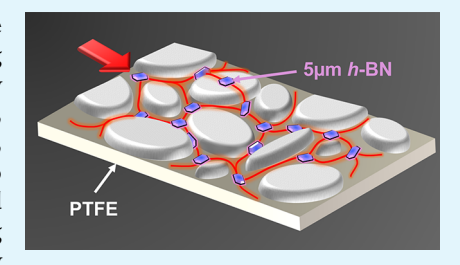
ACCESS I

III Metrics & More



Supporting Information

ABSTRACT: High-temperature polymers are attractive for applications in extreme temperatures, where they maintain their mechanical flexibility and electrical insulating properties. However, their heat dissipation capability is limited due to their intrinsically low thermal conductivities. Hexagonal boron nitride (hBN) is a chemically inert, thermally stable, and electrically insulative compound with a high thermal conductivity, making it an ideal candidate as a filler within a high-temperature polymer matrix to increase the thermal conductivity. This study evaluates the effect of filler size and dispersion on thermal conductivity by producing homogeneous composite samples using a combination of solvent mixing and resonant acoustic mixing (RAM). We carefully



characterized our samples, including the spread of the size distribution, and observed that the smaller sized hBN centered around 5 μ m was able to integrate more seamlessly into the polytetrafluoroethylene (PTFE) matrix with particle size in the 15 μ m range and hence outperformed 30 μ m, in contrast to the conventional wisdom, which asserts that larger fillers universally perform better than smaller ones. Our thermal conductivity of hBN/PTFE composites at 30 wt % is 2× higher than the literature values. Notably, we reached the record-high value of 3.5 W/m K at 40 wt % with an onset of percolation at 20 wt %, attributed to optimized hBN dispersion that facilitates the formation of thermal percolation. Our findings provide general guidelines to enhance the thermal conductivity of polymer composites for thermal management, ranging from power transmission to microelectronics cooling.

KEYWORDS: composites, thermal conductivity, boron nitride, fillers, thermal percolation

1. INTRODUCTION

When considering signal and power transmission, heat dissipation and corrosion/contaminant resistance are crucial in selecting insulating materials. Heat dissipation is of particular concern for high voltage cable efficiency, reliability, and longevity, thereby making high thermal conductivity (k) materials attractive prospects. Most design constraints can be overcome by polymers, but they still fall short in k. Polymer composites can harness the strengths of both the polymer matrix and filler components with added characteristics such as lightweight properties, heightened stiffness, good abrasion resistance, and robust corrosion resistance. 2,3

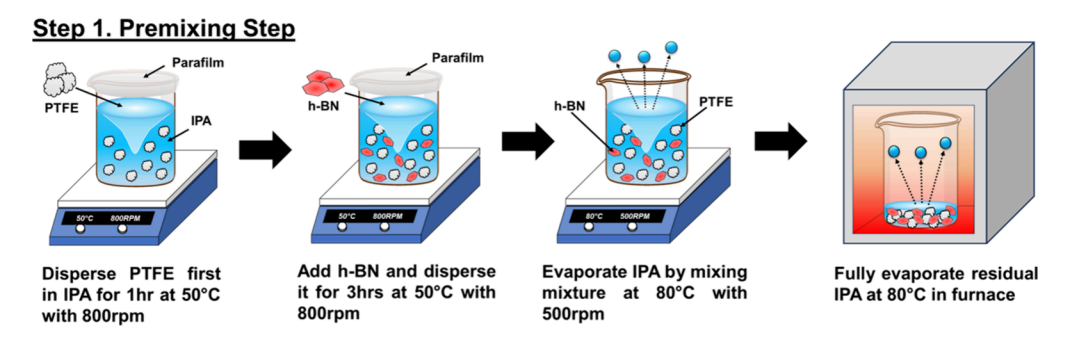
Fluoropolymers, specifically polytetrafluoroethylene (PTFE), feature high thermal stability and chemical inertness with a low dielectric constant, providing a good baseline high-temperature and electrically insulating polymer matrix. However, their k is low, in the typical range from 0.1 to 0.5 W/m K, impeding thermal dissipation. ^{1,4,5} Substantial research efforts have been directed toward enhancing the k values of composite materials by introducing inorganic fillers. These include the integration of carbon nanotubes and graphene, ^{1,6,7} ceramic oxides such as Al_2O_3 and SiO_2 , ^{1,8,9} and nitrides such as BN and AlN. ^{1,10–12} Hexagonal boron nitride (hBN) is particularly of interest due to its notably high intrinsic k in the in-plane direction, ^{1,13} electrical insulation properties,

impressive chemical and thermal stability, and a diminished dielectric constant when compared to materials like Al_2O_3 , SiO_2 , and AlN.^{1,14} Recent work on hBN/PTFE composites has resulted in k values of up to 0.72 W/m K^{15} and 1.14 W/m K^{16} at 30 wt % hBN. These studies used either solid or liquid preparation methods to mix hBN with the polymer matrix and only analyzed composite morphology via SEM after pressing. Detailed hBN size distribution and the level of dispersion were not reported, impeding a thorough understanding of how filler size and dispersion affect the formation of percolation and, thus, k.

In this work, we combined both the liquid and solid phase mixing, liquid mixing occurring within an isopropanol alcohol (IPA) dispersant and solid mixing occurring in a resonant acoustic mixing (RAM) system, to produce a more homogeneous filler distribution within our pressed samples. Note that the application of the RAM process to increase the filler distribution is relatively new. Unlike the traditional mixing

Received: March 6, 2024 Revised: May 15, 2024 Accepted: May 16, 2024





Step 2. Secondary Mixing Step & Sample Hot Pressing

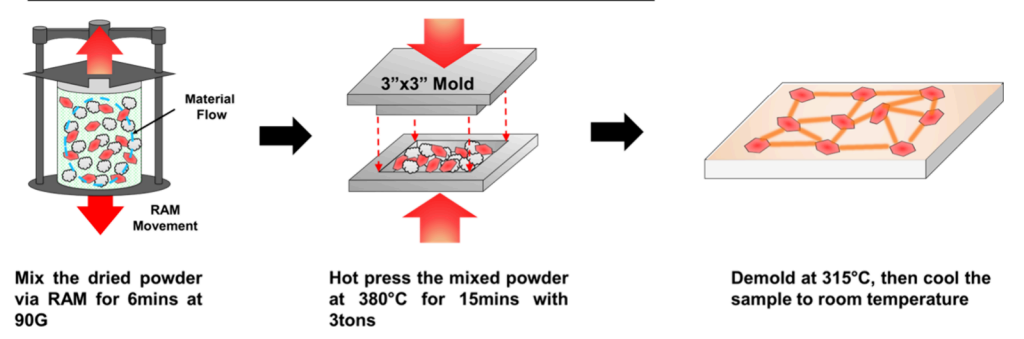


Figure 1. Schematic illustration of the sample premixing and sample fabrication processes. Dispersion of PTFE and hBN filler in organic solvent IPA for liquid-phase mixing and subsequent mixing before pressing using a RAM system to prevent agglomeration and achieve uniformity of the mixed powder.

methods, RAM automatically adjusts the mixing conditions to always operate at a resonance frequency, ensuring thorough mixing. As a result, our composites were able to achieve thermal percolation at 20 wt %, reaching a $2 \times$ higher k at 30 wt % than those seen in hBN/PTFE references, and reached a record-high value of 3.5 W/m K at 40 wt %. Our results highlight the importance of uniform filler dispersion for enhanced k. Laser diffraction analysis (LDA), in addition to SEM, was employed to attain a more accurate measurement of the hBN particle size. In contrast to the conventional wisdom that larger filler sizes gave higher k, we found that a moderately smaller filler size compared to the matrix size facilitates the formation of percolation and results in a larger k. The importance of optimized filler dispersion and the proper particle size to enhance k, as highlighted in this work, is generally applicable to polymer composites. Therefore, our findings offer useful insights for creating thermally conductive polymer composites for high-temperature, electrically insulating applications and, more broadly, for power transmission and microelectronics cooling.

2. METHOD

Preparation of PTFE Composites. PTFE powders were purchased from Goodfellow Cambridge Limited. hBN particles of various size distributions were obtained from Panadyne Inc. As shown in Figure 1, 30 g of PTFE powder was mixed with IPA at 800 rpm and 50 °C using a VWR 7×7 CER Hot plate-Stir 120 V Pro. After 1 h of mixing, hBN particles were added to produce 20, 30, and 40 wt % samples and mixed for 3 h at 50 °C. The IPA evaporation happened when the temperature was increased to 80 °C while the mixing speed was reduced to 500 rpm. As IPA evaporated, the viscosity of the suspension increased, and mixing continued until the suspension thickness exceeded the mixing abilities of the hot plate stirrer. The

sample was then transferred into a Binder Drying and Heating Oven preheated to 80 °C to complete the drying process. Dried hBN/PTFE powders were then RAM mixed at 90G for 6 min to further break up any agglomerates formed during the initial mixing and drying phase. Lastly, the dried composite was pressed using a Wabash MPI G3OH-IS-CX Hot Press. Even with a maximum temperature of 380 °C used in preparation, oxidation is not of concern because hBN nanoparticle oxidation occurs at temperatures above 700 °C. An in-depth explanation of the preparation methodology is provided in the SI.

Characterization. Particle size distribution of hBN powders was measured via LDA (LA-950 Laser Particle Size Analyzer). Scattering data revealed the range of particle sizes present in the samples and their relative abundance. The infrared absorption characteristics of the samples were measured via a Bruker Vertex V80 V Vacuum Fourier-Transform Infrared (FTIR) system. FTIR yielded a highresolution infrared spectrum of the sample's composition. The hBN powder morphology analysis and internal cross-sectional observation of the samples were conducted through a Zeiss Gemini 500 scanning electron microscope (SEM). Sample elemental compositions were determined via analysis of SEM data by using the attached energy-dispersive X-ray spectroscopy (EDS) system. The amount of hBN fillers embedded within the composite materials was confirmed via Thermogravimetric Analysis (TGA). Through the analysis of weight loss profiles at specific temperature ranges and corresponding to the fillers and matrix, it becomes possible to estimate the relative content of fillers within the composite. X-ray diffraction (XRD) measurements were performed by using the Bruker D8 Advanced ECO powder diffractometer. Samples were irradiated with X-rays produced by a 1 kW Cu-K α

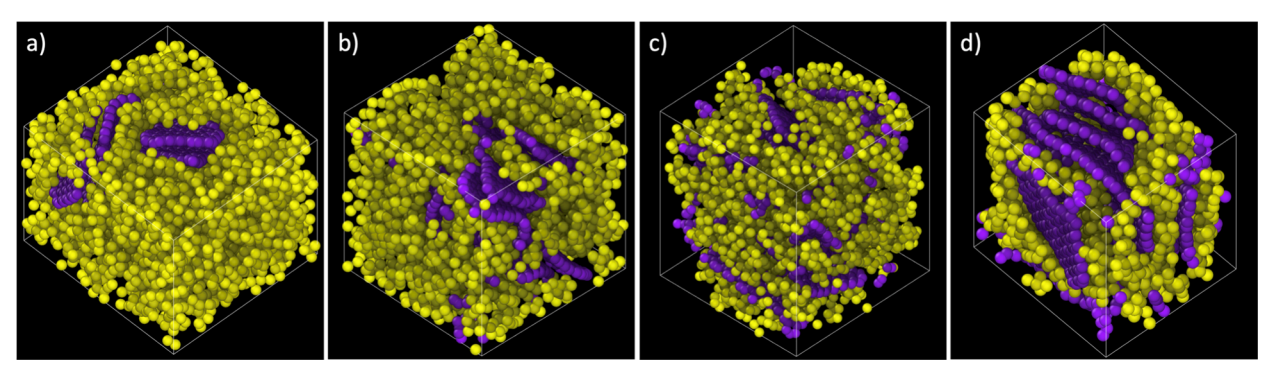


Figure 2. PTFE (yellow) and hBN (purple) composite at 10 wt % (a), 20 wt % (b), 30 wt % (c), and 40% (d) hBN weight percent.

source from various angles to give insight into the chemical structure and functional groups within the composite.

To determine k, which is given by $k = \rho C_v \alpha$, we need the density ρ , heat capacity C_p , and thermal diffusivity α . The thickness and weight of the 1 in. diameter sample were measured by caliper and analytical balance, respectively, and the values were used for density calculation. Thermal diffusivity measurements were performed via the laser flash technique (Linseis XFA 500). The sample's surface was coated with graphite to mitigate surface reflection and improve laser energy absorption. Thermal diffusivity values were taken at 3-5 spots over the same specimen. Heat capacity measurements were obtained through a TA Instruments differential scanning calorimeter (DSC) Auto 2500. To ensure that the small samples measured in DSC are representative of the whole specimen, three positions within each specimen were measured. The average heat capacity was then combined with the thermal diffusivity and density in the subsequent determination of k. An in-depth explanation of the LDA, FTIR, SEM, TGA, Laserflash, DSC, and XRD methods is included in the Supporting Information (SI) document.

Molecular Dynamics Simulations. Equilibrium molecular dynamics simulations $^{17-19}$ were performed to calculate the k of the hBN/PTFE composites. PTFE was first constructed with Materials Studio, and its structure was optimized with the class II polymer consistent force field (PCFF). Since the PCFF cannot calculate the B particle, the structure of hBN nanoparticles was optimized by the universal force field. An amorphous cell calculation was then initiated with the geometrically optimized PTFE and hBN, in which the initial density of the amorphous cell calculation was set at 2.2 g/cm³. hBN/PTFE composites from 0 to 40 wt % hBN weight percent were constructed, and as an example, the cell size of the 40 wt % BhN weight percent composite was 37.9 Å × 37.9 Å × 37.9 Å, as visualized with OVITO in Figure 2.

Once the atomic positions were determined from Materials Studio, the LAMMPS input file was created. In LAMMPS, a hybrid interatomic potential was used, in which the PTFE was modeled with the PCFF and the BN with the Extended Tersoff potential (BN-ExTEP).²³ The BN-ExTEP accurately describes the main low energy B, N, and hBN structures and yields quantitively correct trends in bonding as a function of coordination.²³ Since the BN-ExTEP is employed for monolayers, we modeled the interactions between hBN layers with the LJ potential to account for the vdW interactions. The system was relaxed in isothermal—isobaric (NPT), canonical (NVT), and microcanonical (NVE) ensembles subsequently for 100, 50, and 50 ps, respectively, and then heat flux data was

collected in an NVE ensemble for another 1 ns. The k was determined with the Green–Kubo formula, which relates the ensemble average of the autocorrelation of the heat flux to k^{24-27}

3. RESULTS AND DISCUSSION

Before the composites were synthesized, hBN particle sizes were confirmed using LDA methods and SEM measurements. After we obtained hBN/PTFE composites, we confirmed the chemical composition and percentage using FTIR, TGA, and XRD. Further composition and structural analysis were carried out via SEM and EDS system while thermal conductivity was calculated using a combination of laser flash and DSC measurements. The detailed results from XRD, FTIR, and TGA measurements are included in the SI.

Thermal Conductivity. The *k* is determined by $k = \rho C_n \alpha$, where ρ is the density, C_p is the heat capacity, and α is the thermal diffusivity. Figure 3a shows the nearly constant heat capacity of around 1.5 J/(g K) throughout all filler contents investigated, regardless of particle sizes. As shown in Figure 3b, the density was fairly constant. As depicted in Figure 3c, thermal diffusivity increased with the increasing hBN content for both SP5 and SP30 (particle size centered around 5 and 30 μ m, respectively), with a rapid surge in thermal diffusivity initiating at approximately 20 wt %. Then, we calculated k, as shown in Figure 3d. Given that the density and heat capacity remained relatively constant with increasing hBN loading, k mainly followed the trend of thermal diffusivity. If no percolation was prevalent, then the increasing k with increasing hBN weight percentage trend should be linear. This is supported by molecular dynamics simulations with the highest k value of 1.41 W/m K obtained at 40 wt %, as shown in Figure 3d. Interestingly for both SP5 and SP30, k not only increases with increasing hBN weight percentage, as expected, but we also observe the superliner region, the hallmark of

Effects of Filler Size. The literature 14,28 generally reported a larger filler particle size results in a higher composite k at the same filler content. However, we observed that otherwise. A deeper dive into the actual hBN particle sizes and the PTFE particle sizes revealed that (with both PTFE and filler particles on the microscale) the relative size between the filler and matrix, rather than the absolute size of the filler, matters more: with the PTFE particle size lying in the 15 μ m range, the smaller SP5 hBN is able to more evenly distribute and fit inbetween PTFE aiding the homogeneous incorporation into the pressed composite matrix, facilitating its formation of a uniform percolation network.

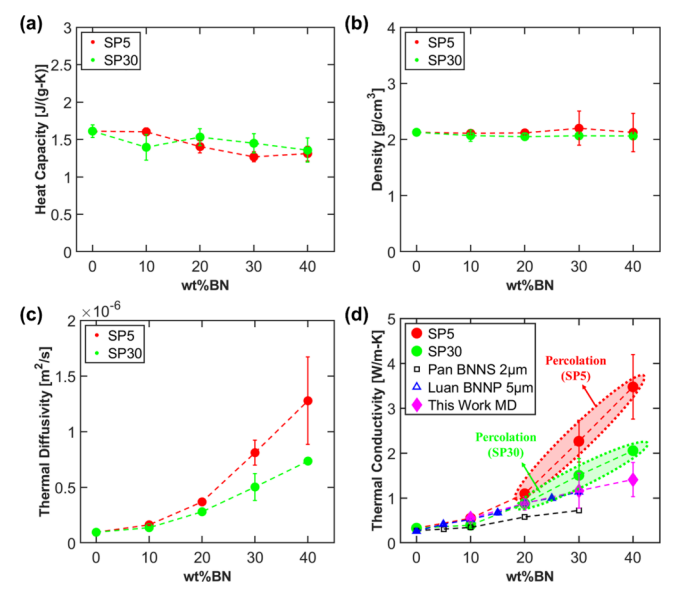


Figure 3. (a) Heat capacity measurements determined by DSC as a function of hBN filler content. (b) Measured density indicates a nearly constant value, with an average ranging from 2.0 to 2.2 g/cm^3 . (c) Thermal diffusivity measured with a laser flash method (XFA 500). A rapid surge in diffusivity initiates at 20 wt % hBN. (d) k calculated using the measured data in panels (a)—(c). Up to 20 wt % hBN, the k values follow a similar trend as our own MD results and experimental data in the literature; however, analysis shown later in the paper suggests that beyond 20 wt % hBN, the increase in k values is due to the formation of thermal percolation networks in both SPS and SP30 cases.

Typically, the observation of commercial hBN particle size distribution is determined by comparing SEM images to the manufacturer datasheets. In this study, we took an additional step to confirm the manufacturer's provided size distribution via LDA of around 2 g of hBN powders, in addition to SEM. Our SEM measurements of hBN powders, Figure 4a,b, and our

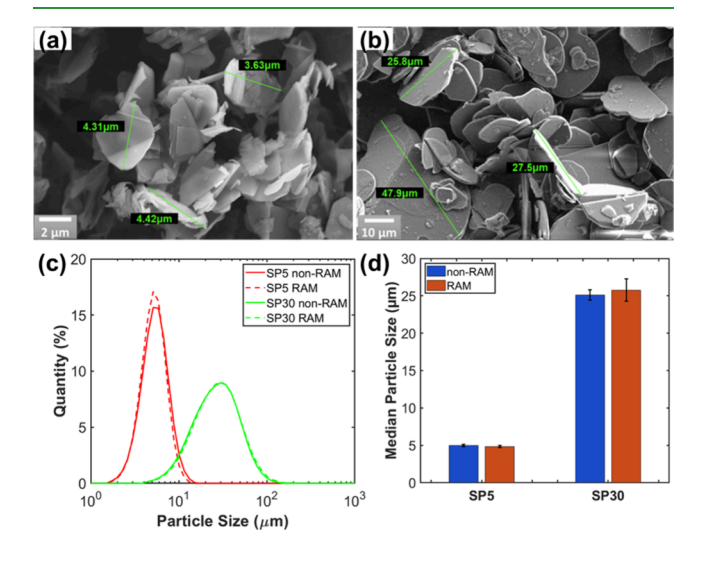


Figure 4. SEM of Panadyne hBN powders before RAM and the particle size analyzer of hBN powder before and after RAM: (a) SP5 SEM and (b) SP30 SEM. LDA results on (c) distribution of particle sizes for hBN SP5 and SP30 obtained via LDA and (d) mean particle size for hBN SP5 and SP30 RAM and non-RAM cases obtained via LDA. RAM mixing at 90G for 6 min did not break the hBN particles.

particle size distribution from LDA, Figure 4c,d, both indicated a consensus with manufacturer datasheets.". Notably, RAM mixing at 90G for 6 min did not affect the hBN particle sizes. Analysis of PTFE powders was attempted using LDA methods; however, particles tended to agglomerate once they were placed in solution, yielding inaccurate results. SEM analysis of PTFE powders after RAM mixing shows an average size of around 15 μ m, a 25% reduction from the manufacturer-provided average size of 20 μ m. These 15 μ m PTFE particles are 3× larger than the SP5 particles, allowing for a better BN incorporation between and around PTFE than SP30 particles, whose size is larger than PTFE particles. The relatively smaller filler is thus beneficial for forming a uniform percolation network and achieving a higher k.

To further confirm this hypothesis, we took a close look at the hBN and PTFE networks within composite samples using SEM/EDS analysis. This meticulous examination involved cryogenic fracturing of the specimen using liquid nitrogen, which allowed for detailed observation of its cross section. As shown in Figure 5, the cross sections of two samples with different particle sizes were observed with SEM to confirm the network of hBN and PTFE. The elemental spectra of hBN, consisting of boron (B) and nitrogen (N), and the spectra of PTFE, consisting of carbon (C) and fluorine (F), were also confirmed using EDS.

Regarding the smaller particle size, SP5, hBN platelets displayed a random orientation, forming a well-dispersed network through interconnection with individual PTFE fibers and the bulk PTFE matrix, as shown in Figure 5a. On the other hand, hBN platelets of the larger particle size, SP30, were generally stacked in one direction and formed platelet aggregates embedded in the PTFE matrices, as shown in Figure 5b. Hence, hBN platelets with smaller particle sizes demonstrated a notably more harmoniously integrated and better dispersion within the PTFE matrices with diverse orientations. SP30 particles at each wt % showed an increased prevalence of agglomeration within the PTFE matrix when compared with SP5 samples. In other words, the smaller particles' ability to integrate better in between the PTFE matrix compared to the larger particles facilitated the formation of the uniform percolation network. This results in the highest seen *k* value of 3.5 W/m K obtained in the 40 wt % SP5 sample. For SP30, it may have formed a partial network. Mixtures of hBN particle sizes were shown to outperform either smaller or larger particles in the literature. Thus, we mixed SP5, SP12, and SP30 hBN (in a 1:1:1 ratio) to observe the effects on the thermal conductivity. The mixed samples performed in the same range as SP30 samples and consistently worse than SP5 samples, with 30% achieving a k of 1.28 W/m K and a maximum k of 2.03W/m k seen at 40%. SEM micrographs in the SI also show larger particles significantly stand out from the bulk PTFE matrix compared to SP5 samples

If we compare our results with the hBN/PTFE literature, where PTFE with an average particle size of 50 μ m^{15,16} and hBN with average sizes between 100 nm and 5 μ m^{15,16} were used, and a much lower k was obtained, it reiterates the importance of having improved size compatibility in PTFE and hBN to enhance k.

Effect of Filler Dispersion. Differences in mixing methods – specifically the addition of RAM – can be accounted as another key factor between hBN/PTFE references and this study, which yielded a 2\AA higher k value. Prior works used either mixing in the solid phase (not RAM mixing) or a two-

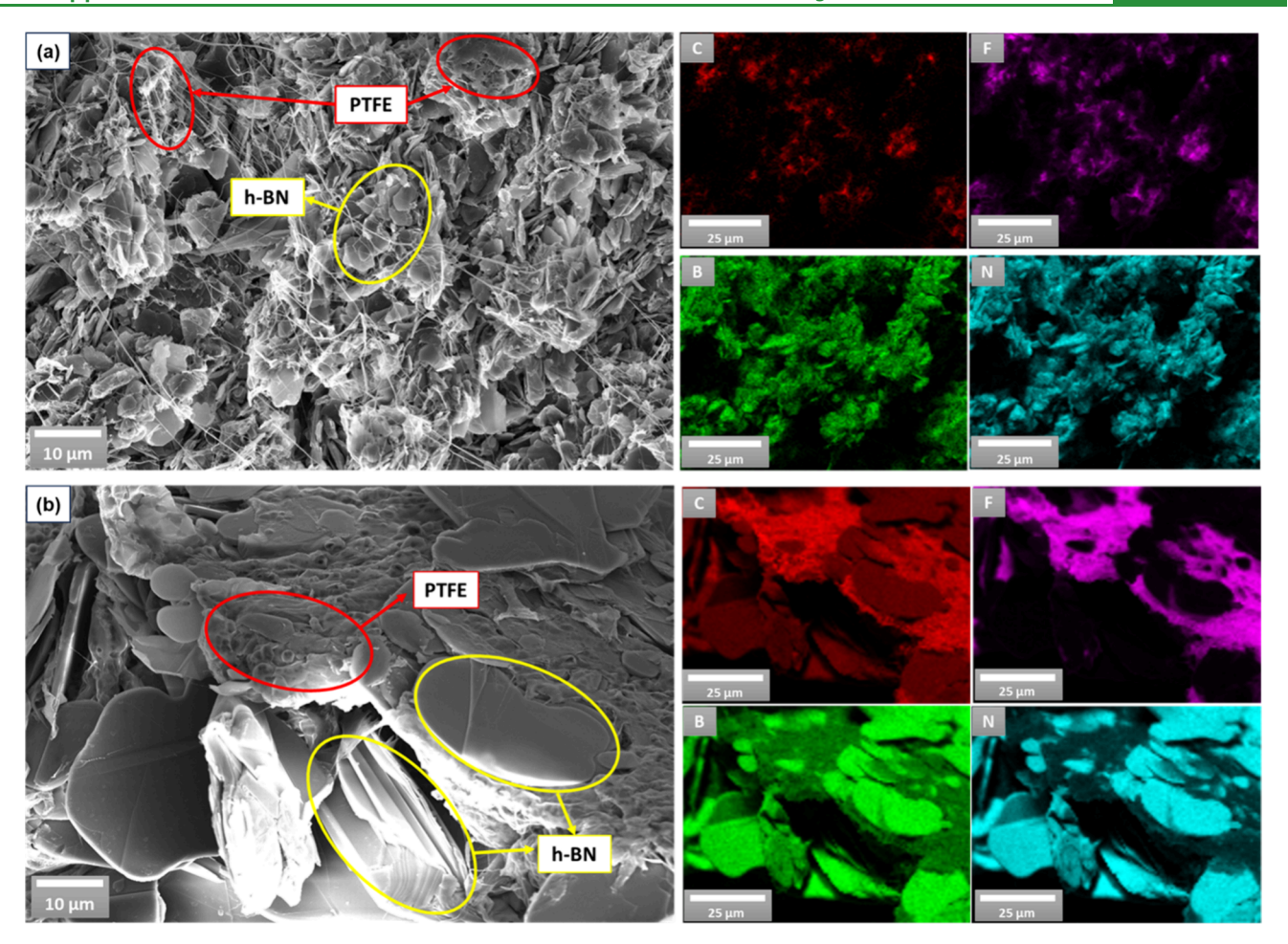
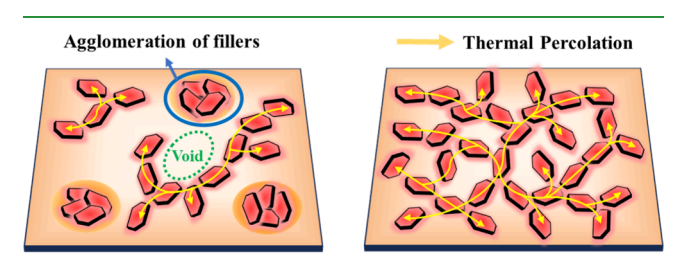


Figure 5. SEM/EDS of a cross-sectional view of hBN/PTFE composites. (a) Cross-sectional view of SP5; PTFE matrices and fibers network compactly with hBN platelets; (b) cross-sectional view of SP30; hBN platelets stack together and form platelet aggregates that embed into PTFE matrices.

step liquid mixing process that dispersed PTFE and hBN in acetone via sonication. Our process combined both solid and liquid mixing techniques by using a three-step liquid mixing process: mixing PTFE in IPA, adding hBN and mixing, and evaporating IPA while mixing, and then drying in an oven before RAM mixing. Due to the insolubility of both hBN and PTFE in most solvents and their tendency to form agglomerates rather than homogeneous dispersions in solution, previous studies on hBN/PTFE were unable to reach the percolation. Agglomerates were also seen in our previous samples made without the use of RAM methods (see SI). The application of RAM reduced the size of any agglomerates leftover from premixing and ensured even distribution of dried hBN and PTFE particles. This focus on agglomerate size reduction allowed us to achieve a better dispersion and uniform distribution of particles within the PTFE matrix and, therefore, assist in forming the observed percolation network, enhancing k. With other polymer matrices, hBN-based composites were easier to achieve percolation. Nevertheless, our k is still record-high -25% higher than the highest hBN/ polypropylene(PP)²⁹ sample and 100% higher than the highest BN/silicone²⁸ at 30% BN. Note that although RAM mixing is important, the premixing step is also crucial to achieve uniform mixing. One of the key innovations of this work lies in the combination of premixing and RAM mixing.

Homogeneous distribution is critical to achieving thermal percolation, as illustrated in Figure 6. Given the same filler



Inhomogeneous Distribution Homogeneous Distribution

Figure 6. (a) Inhomogeneous mixing results in hBN particle agglomeration and voids that prevent the formation of percolation. (b) homogeneous mixing of smaller particles leads to the development of thermal pathways and percolation networks to achieve a high

content, improper preparation leads to inhomogeneous distribution and agglomerated fillers, leaving voids that prevent the formation of a continuous filler network: thermal percolation pathways. In contrast, a homogeneous distribution is the easiest way to form thermal percolation.

k value.

5. CONCLUSIONS

Our investigation of the thermal conductivity of polymer composites, specifically SP5 and SP30 with varying hBN contents, revealed relationships between thermal conductivity and filler loading, size, and dispersion. Molecular dynamics simulations displayed a linear increasing trend in thermal conductivity with hBN weight percentage, with the highest thermal conductivity value of 1.41 W/m K obtained at 40 wt %, indicating no prevalent percolation, probably due to the limited particle size and simulation domain size. Measured thermal diffusivity, and consequently thermal conductivity, demonstrated a linear trend at lower filler loading, followed by a deviation into the superlinear regime at approximately 20 wt %, suggesting that percolation transport begins to take effect and resulting in 2× higher thermal conductivity at 30 wt % and a significantly high thermal conductivity value of 3.5 W/m K achieved at 40 wt % SP5. Achievement of the higher thermal conductivity compared to the literature and the thermal conductivity percolation regime can be attributed to two significant distinctions: uniform particle dispersion via a combination of liquid-phase premixing and solid-phase RAM mixing and careful filler selection that allows a slightly smaller filler to be better incorporated into the matrix. Our findings provide general guidelines to enhance the thermal conductivity of polymer composites for thermal management, ranging from power transmission to microelectronics cooling.

ASSOCIATED CONTENT

5 Supporting Information

The Supporting Information is available free of charge at https://pubs.acs.org/doi/10.1021/acsami.4c03818.

Supporting Information includes detailed sample preparation information, descriptions of all characterization methods employed and results from x-ray diffraction (XRD) and Fourier-transform infrared (FTIR) analysis; data and pictures of non-RAM samples are also included. (PDF)

AUTHOR INFORMATION

Corresponding Author

Zhiting Tian — Cornell University Sibley School of Mechanical and Aerospace Engineering, Cornell University, Ithaca, New York 14853, United States; Occid.org/0000-0002-5098-7507; Email: zt223@cornell.edu

Authors

- Liam Alexis Cornell University Sibley School of Mechanical and Aerospace Engineering, Cornell University, Ithaca, New York 14853, United States; orcid.org/0000-0002-7075-1438
- Jaejun Lee Cornell University Department of Materials Science and Engineering, Cornell University, Ithaca, New York 14853, United States
- Gustavo A. Alvarez Cornell University Sibley School of Mechanical and Aerospace Engineering, Cornell University, Ithaca, New York 14853, United States
- Samer Awale Cornell University Department of Materials Science and Engineering, Cornell University, Ithaca, New York 14853, United States
- Diana Santiago-de Jesus NASA Glenn Research Center, Cleveland, Ohio 44135, United States

Maricela Lizcano – NASA Glenn Research Center, Cleveland, Ohio 44135, United States

Complete contact information is available at: https://pubs.acs.org/10.1021/acsami.4c03818

Notes

The authors declare no competing financial interest.

ACKNOWLEDGMENTS

This work is supported by NASA ESI Award 80NSSC22K0261. The authors acknowledge the use of facilities and instrumentation supported by NSF through the Cornell University Materials Research Science and Engineering Center DMR-1719875.

REFERENCES

- (1) Hou, J.; Li, G.; Yang, N.; Qin, L.; Grami, M. E.; Zhang, Q.; Wang, N.; Qu, X. Preparation and characterization of surface modified boron nitride epoxy composites with enhanced thermal conductivity. *RSC Adv.* **2014**, *4* (83), 44282–44290.
- (2) Camargo, P. H. C.; Satyanarayana, K. G.; Wypych, F. Nanocomposites: synthesis, structure, properties and new application opportunities. *Mater. Res.* **2009**, *12* (1), 1–39.
- (3) Joy, J.; George, E.; Haritha, P.; Thomas, S.; Anas, S. An overview of boron nitride based polymer nanocomposites. *J. Polym. Sci.* **2020**, 58 (22), 3115–3141.
- (4) Huang, X.; Jiang, P.; Tanaka, T. A review of dielectric polymer composites with high thermal conductivity. *IEEE Electrical Insulation Magazine* **2011**, 27 (4), 8–16.
- (5) Wei, X.; Wang, Z.; Tian, Z.; Luo, T. Thermal Transport in Polymers: A Review. J. Heat Transfer 2021, 143 (7), No. 072101.
- (6) Morishita, T.; Matsushita, M.; Katagiri, Y.; Fukumori, K. Noncovalent functionalization of carbon nanotubes with maleimide polymers applicable to high-melting polymer-based composites. *Carbon* **2010**, 48, 2308 DOI: 10.1016/j.carbon.2010.03.007.
- (7) Kim, H.; Lu, K.; Liu, Y.; Kum, H. S.; Kim, K. S.; Qiao, K.; Bae, S. H.; Lee, S.; Ji, Y. J.; Kim, K. H.; Paik, H.; Xie, S.; Shin, H.; Choi, C.; Lee, J. H.; Dong, C.; Robinson, J. A.; Lee, J. H.; Ahn, J. H.; Yeom, G. Y.; Schlom, D. G.; Kim, J. Impact of 2D-3D Heterointerface on Remote Epitaxial Interaction through Graphene. *ACS Nano* **2021**, *15* (6), 10587–10596.
- (8) Hong, J.; Lee, J.; Jung, D.; Shim, S. E. Thermal and electrical conduction behavior of alumina and multiwalled carbon nanotube incorporated poly(dimethyl siloxane). *Thermochim. Acta* **2011**, *512* (1–2), 34–39.
- (9) Ren, L.; Pashayi, K.; Fard, H. R.; Kotha, S. P.; Borca-Tasciuc, T.; Ozisik, R. Engineering the coefficient of thermal expansion and thermal conductivity of polymers filled with high aspect ratio silica nanofibers. *Compos B Eng.* **2014**, *58*, 228–234.
- (10) Gu, J.; Zhang, Q.; Ďang, J.; Xie, C. Thermal conductivity epoxy resin composites filled with boron nitride. *Polym. Adv. Technol.* **2012**, 23 (6), 1025–1028.
- (11) Qian, R.; Yu, J.; Xie, L.; Li, Y.; Jiang, P. Efficient thermal properties enhancement to hyperbranched aromatic polyamide grafted aluminum nitride in epoxy composites. *Polym. Adv. Technol.* **2013**, 24 (3), 348–356.
- (12) Williams, T.; Nguyen, B.; Fuchs, W., "Polyphenylsulfone-hBN Composite Insulation," *Proceedings of the 2020 IEEE 3rd International Conference on Dielectrics (ICD)*; 2020, 541–545 (2020).
- (13) Huang, M. T.; Ishida, H. Investigation of the Boron Nitride/Polybenzoxazine Interphase. *J. Polym. Sci. B: Polym. Phys.* **1999**, 37, 2360–2372.
- (14) Li, T. L.; Hsu, S. L. C. Enhanced thermal conductivity of polyimide films via a hybrid of micro- and nano-sized boron nitride. *J. Phys. Chem. B* **2010**, *114* (20), 6825–6829.
- (15) Pan, C.; Kou, K.; Zhang, Y.; Li, Z.; Wu, G. Enhanced throughplane thermal conductivity of PTFE composites with hybrid fillers of

- hexagonal boron nitride platelets and aluminum nitride particles. *Composites, Part B* **2018**, *153*, 1–8, DOI: 10.1016/j.compositesb.2018.07.019.
- (16) Luan, B. C. D.; Huang, J.; Zhang, J. Enhanced thermal conductivity and wear resistance of polytetrafluoroethylene composites through boron nitride and zinc oxide hybrid fillers. *J. Appl. Polym. Sci.* **2015**, *132* (30), 42302.
- (17) Ma, H.; Tian, Z. Significantly High Thermal Rectification in an Asymmetric Polymer Molecule Driven by Diffusive versus Ballistic Transport. *Nano Lett.* **2018**, *18* (1), 43–48.
- (18) Ma, H.; Aamer, Z.; Tian, Z. Ultrahigh thermal conductivity in three-dimensional covalent organic frameworks. *Mater. Today Phys.* **2021**, *21*, No. 100536, DOI: 10.1016/j.mtphys.2021.100536.
- (19) Ma, H.; O'Donnel, E.; Tian, Z. Tunable thermal conductivity of π -conjugated two-dimensional polymers. *Nanoscale* **2018**, *10*, 13924.
- (20) Sun, H. Ab Initio Calculations and Force Field Development for Computer Simulation of Polysilanes. *Macromolecules* **1995**, 28, 701–712.
- (21) Casewit, C. J.; Colwell, K. S.; Rappé, A. K. Application of a Universal Force Field to Main Group Compounds. *J. Am. Chem. Soc.* **1992**, *114* (25), 10046–10053.
- (22) Rappe, A. K.; Casewit, C. J.; Colwell, K. S.; Goddard, W. A.; Skiff, W. M. UFF, a Full Periodic Table Force Field for Molecular Mechanics and Molecular Dynamics Simulations. *J. Am. Chem. Soc.* 1992, 114 (25), 10024.
- (23) Los, J. H.; Kroes, J. M. H.; Albe, K.; Gordillo, R. M.; Katsnelson, M. I.; Fasolino, A. Extended Tersoff potential for boron nitride: Energetics and elastic properties of pristine and defective h-BN. *Phys. Rev. B* **2017**, *96*, No. 184108.
- (24) Ikeshoji, T.; Hafskjold, B. Non-equilibrium molecular dynamics calculation of heat conduction in liquid and through liquid-gas interface. *Mol. Phys.* **1994**, *81* (2), 251–261.
- (25) Li, C.; Ma, H.; Li, T.; Dai, J.; Rasel, M. A. J.; Mattoni, A.; Alatas, A.; Thomas, M. G.; Rouse, Z. W.; Shragai, A.; Baker, S. P.; Ramshaw, B. J.; Feser, J. P.; Mitzi, D. B.; Tian, Z. Remarkably Weak Anisotropy in Thermal Conductivity of Two-Dimensional Hybrid Perovskite Butylammonium Lead Iodide Crystals. *Nano Lett.* **2021**, *21* (9), 3708–3714.
- (26) Ma, H.; Li, C.; Tian, Z. Hydrogen Bonds Significantly Enhance Out-of-Plane Thermal and Electrical Transport in 2D Graphamid: Implications for Energy Conversion and Storage. *ACS Appl. Nano Mater.* **2020**, 3 (11), 11090–11097.
- (27) Ma, H.; Babaei, H.; Tian, Z. The importance of van der Waals interactions to thermal transport in Graphene-C60 heterostructures. *Carbon* **2019**, *148*, 196 DOI: 10.1016/j.carbon.2019.03.076.
- (28) Zhou, W. Y.; Qi, S. H.; Zhao, H. Z.; Liu, N. L. Thermally conductive silicone rubber reinforced with boron nitride particle. *Polym. Compos* **2007**, 28 (1), 23–28.
- (29) Cheewawuttipong, W.; Fuoka, D.; Tanoue, S.; Uematsu, H.; Iemoto, Y. Thermal and Mechanical Properties of Polypropylene/Boron Nitride Composites. *Energy Procedia* **2013**, *34*, 808–817.